



HAL
open science

Glass forming regions, structure and properties of lanthanum barium germanate and gallate glasses

Florian Calzavara, Mathieu Allix, Marc Dussauze, Veronique Jubera, Marcelo Nalin, Thierry Cardinal, Evelyne Fargin

► **To cite this version:**

Florian Calzavara, Mathieu Allix, Marc Dussauze, Veronique Jubera, Marcelo Nalin, et al.. Glass forming regions, structure and properties of lanthanum barium germanate and gallate glasses. *Journal of Non-Crystalline Solids*, 2021, 571, pp.121064. 10.1016/j.jnoncrysol.2021.121064 . hal-03365080

HAL Id: hal-03365080

<https://hal.science/hal-03365080>

Submitted on 5 Oct 2021

HAL is a multi-disciplinary open access archive for the deposit and dissemination of scientific research documents, whether they are published or not. The documents may come from teaching and research institutions in France or abroad, or from public or private research centers.

L'archive ouverte pluridisciplinaire **HAL**, est destinée au dépôt et à la diffusion de documents scientifiques de niveau recherche, publiés ou non, émanant des établissements d'enseignement et de recherche français ou étrangers, des laboratoires publics ou privés.

*Glass forming regions, structure and properties of lanthanum barium
germanate and gallate glasses*

Florian Calzavara^{a*}, Mathieu Allix^b, Marc Dussauze^c, Véronique Jubera^a, Marcelo Nalin^d,
Thierry Cardinal^a, Evelyne Fargin^a

^a Institut de Chimie de la Matière Condensée de Bordeaux, Université de Bordeaux, 87 Avenue du Dr Schweitzer, Pessac F-33608, France

^b Conditions Extrêmes et Matériaux : Haute Température et Irradiation, UPR3079, Université d'Orléans, 1 Avenue de la Recherche Scientifique, 45100 Orléans, France

^c Institut des Sciences Moléculaires, UMR 5255, Université de Bordeaux, 351 cours de la Libération, Talence Cedex 33405, France

^d Institute of Chemistry – São Paulo State University-UNESP, Rua Prof. Francisco Degni, 55, CEP 14800-060, Araraquara -SP, Brazil

*Corresponding author: florian.calzavara@icmcb.cnrs.fr

Abstract

Glass forming regions in the system $\text{GaO}_{3/2} - \text{GeO}_2 - \text{LaO}_{3/2} - \text{BaO}$ have been explored using aerodynamic levitation coupled to laser heating synthesis technique. Structure property relationships have been established between the thermal and optical properties of the resulting glass thanks to Raman and Infrared vibrational spectroscopies. The germano-gallate glass networks are mainly made of three-dimensional interconnected corner shared GeO_4 and GaO_4 tetrahedra forming $\text{Ge} - \text{O} - \text{Ge}$ and $\text{Ga} - \text{O} - \text{Ge}$ bridges in which gallium tetrahedral GaO_4 units are charged-compensated by barium and lanthanum cations. In GeO_2 -rich compositions, the excess of positive charges produces mainly non-bridging oxygens on germanate moieties, leading to a depolymerization of the glass network. In the case of gallium rich compositions, the infrared cut-off is red-shifted as compared to the germanate glasses, in accordance with the disappearance of germanium associated entities such as germanium and gallium bridges or germanium sites with non-bridging oxygen both vibrating at higher wavenumber.

Keywords: heavy-metal oxide glasses, germano-gallate glasses, glass structure, vibrational Infrared and Raman spectroscopies, aerodynamic levitation coupled to laser heating.

Introduction

Novel mid-infrared (MIR) transparent materials are attracting attention for the development of all on-chip photonic devices either as active or passive components [1]. Being transparent in the fingerprint window of various molecular species, they offer the possibility to easily detect traces of environmental gases and toxic vapors, such finding a variety of applications in health [2], environment, atmospheric, telecommunication and defense or security. Vitreous systems based on heavy metal oxide (HMO) are particularly of interest since they can be readily shaped with reasonable costs, providing a mechanically robust and chemically durable alternative to fluoride and chalcogenide glasses, even though their transparent window extension towards the mid-IR remains less extended. Compared with common oxide glass systems such as (alumino-)silicates, borates or phosphates, HMO glasses possess a large transmission window ranging from the ultraviolet domain to mid-infrared (transmission cut-off up to $\sim 8 \mu\text{m}$) [3]. They also exhibit a relatively high third order polarizability which make HMO glasses suitable for nonlinear applications [4]. In the past, bismuthate-, lead-, scandium-, thallium- germanate-based [5] or gallate-based [3], [4], [6]–[20] glasses were particularly investigated. However, the toxicity of some constituent may limit their use. Barium germano-gallate (BGG) glasses have been alternatively developed following the pioneer work of Higby [21], emphasizing their usefulness for optical components such as low-loss optical fibers [21] or bulk optics [22]–[25]. The introduction of either low field cations (*i.e.* alkaline-earth MO or alkaline M_2O) or by substituting barium oxide into the modified BGG low phonon glass systems have been recently investigated [24], [25]. The glass network is reported to be formed of 3D tetrahedral sites of oxygenated germanium and gallium in which the alkaline earth and alkali compensate the gallium tetrahedral negative charge. We have previously reported that such compositions tend to lead to strong surface crystallization [26], [27], making difficult the development of waveguiding optical fibers for instance using preform based technologies [24] [25].

Alternatively, the introduction of high field rare-earth (RE) components in germano-gallate glasses has been little explored even if fiber drawing has been reported [28]–[33]. Introduction of rare-earth ions for laser applications are of importance and requires to investigate the effect of rare-earth introduction on the glass structure and properties. Following our previous works, here we explore the multicomponent glass forming diagram $\text{GaO}_{3/2} - \text{GeO}_2 - \text{BaO} - \text{LaO}_{3/2}$ while varying the barium oxide content from zero up to twenty cationic molar percent. Main relationships between physical, thermal and structural properties will be discussed. The investigation of the vitreous domain was explored using aerodynamic levitation coupled to laser heating (ADL) to access high melting temperatures and fast quenching rates with a contactless approach to avoid heterogeneous crystallisation. The melts were reproduced in most cases using classical melt-quenching techniques in order to obtain centimeter size samples. Nonetheless, glasses with no germanium oxide could not be obtained using traditional melt quenching technique. Vibrational spectroscopies have been investigated in order to establish composition/structure/properties relationships.

Experimental procedure

Glasses were elaborated using high purity powders Ga_2O_3 (Fox Chemicals, $\leq 99.999\%$), GeO_2 (Fox Chemicals, $\leq 99.999\%$), La_2O_3 (Stream Chemicals, $\leq 99.99\%$) and BaCO_3 (Fox Chemicals, $\leq 99.99\%$). The

mixtures were then grinded and pressed into pellets before being placed in the ADL setup. Melting temperatures between ~ 1450 °C and ~ 1700 °C were attained using two CO₂ lasers with an operating wavelength of $\lambda = 10.6$ μm . An argon flux was used to levitate the melted sphere during the whole synthesis process. The spherical melt was homogenized during a few seconds. Samples of 3 mm diameter were successively quenched down to room temperature by shutting down the laser power. Spherical, transparent and colorless glasses were been obtained as shown in Figure 1e. No further thermal annealing was performed. Finally, the samples were cut and polished on both parallel faces for further characterizations. The compositions have been normalized as follow: $x \text{ GaO}_{3/2} + y \text{ GeO}_2 + z \text{ LaO}_{3/2} = 100$ cationic molar percentage (cationic mol %) where x, y and z correspond, respectively, to the gallium, germanium and lanthanum oxides cationic molar percentages.

Physical and thermal characterizations.

Thermal properties including the onset of glass transition temperature (T_g) and the onset of crystallization (T_x) were measured on a Netzsch DSC Pegasus 404 F3 apparatus in a platinum pan using glass chunks of about 10 – 20 mg. A heating rate of 10 °C.min⁻¹ has been used. The onset of T_g and T_x were determined from the DSC trace from the tangents crossing. The error has been estimated to be equal to ± 4 °C. The density ρ was obtained from the average of five measurements per sample using Archimedes' method by immersing a glass chunk in diethyl phthalate at room temperature on a Precisa XT 220A weighing scale. The estimated errors were estimated around ± 0.01 g.cm⁻³.

Optical properties have been investigated by transmission measurements. The extinction coefficient α has been deduced from the transmission spectra according to the relation $\alpha = -\frac{\ln(I/I_0)}{x}$, where x is the sample's thickness and I/I_0 the transmission percentage. In this case, we assume that the extinction coefficient can be considered as the absorption coefficient due to negligible scattering in the samples. The infrared transmission spectra were recorded on a spectrometer Brüker Equinox 55 from 4000 cm⁻¹ to 1000 cm⁻¹ with a spectral resolution of 4 cm⁻¹. The spectra have been recorded from an average of 128 scans. The ultraviolet– visible transmission spectra were recorded on a Cary5000 (Varian) from 200 nm to 2500 nm with a spectral resolution of 1 nm.

Structural characterizations by vibrational spectroscopies.

Unpolarized Raman spectra were recorded with a confocal micro-Raman spectrometer LabRAM HR Evolution (Horiba Jobin Yvon) equipped with a Synapse CCD detector cooled down to -70 °C using a 532 -nm radiation from a diode pumped solid state laser (output power = 20 mW). The incident laser beam was focused onto the sample through a microscope with a $50\times$ objective (NA = 0.50 , Olympus). Scattered light was dispersed by 1200 grooves. mm⁻¹ grating system. Raman spectra have been corrected by the Bose-Einstein factor. They have then been normalized between 400 cm⁻¹ and 1000 cm⁻¹ with respect to the maximum intensity peak located in the low frequency range defined as $400 - 600$ cm⁻¹.

Reflectance infrared spectra have been recorded with an incident angle of 11° from 200 to 1500 cm⁻¹ with a spectral resolution of 4 cm⁻¹ using a Fourier Transform Spectrometer Vertex 70 V. A mid-infrared source has

been used (global type). All measurements were performed in vacuum. The spectra have been averaged from three measurements of 200 scans each. Kramers-Kronig transforms have been performed in order to extract the extinction coefficient k from the imaginary part of the refractive index \underline{n} according to the relation $\underline{n} = n_0 + i k$ with n_0 the linear refractive index.

Results

The obtained glass formation domains explored using aerodynamic levitation melting process are reported in Figure 1. We focused the investigation on the main network former domain corresponding to germanium and gallium oxides-rich compositions as depicted in Figure 1. Under our synthesis conditions, we report in Figure 1a-d the glass forming regions in the multicomponent system $(1 - \alpha) (x \text{GaO}_{3/2} - y \text{GeO}_2 - z \text{LaO}_{3/2}) - \alpha \text{BaO}$ for four fixed values of the barium oxide content α ranging from zero up to twenty cationic molar percent ($\alpha = 0, 10, 16, 20$). The vitreous domain for the barium-free diagram (Figure 1a) corresponds to germanate-type glasses in which the germanium oxide content ranges from about $\sim 30\%$ up to $\sim 65\%$ GeO_2 cationic molar percent. The reported diagram is in relatively good accordance with the work already described by several authors [28], [29] and by Hwa *et al.*[29], [34]. When 10% of barium oxide content is added (Figure 1b), the vitreous domain is extended to the richest germanium oxide-containing glasses and in the region with the lowest lanthanum oxide amount. Gallate-rich and germanium-free glasses can be also synthesized. The region corresponding to gallium concentrations up to $\sim 75\%$ of $\text{GaO}_{3/2}$ content was not explored. With 16% of barium oxide content in the $\text{Ga}_2\text{O}_3 - \text{GeO}_2 - \text{La}_2\text{O}_3$ system, a similar glass forming region (Figure 1c) as compared with the region with 10 cationic percent of barium oxide is obtained. For 20 cationic percent of barium oxide introduced, a shrink of the vitreous domain occurs with in particular no glass formation in the gallium-rich and the lanthanum-rich region.

The relationships between the glass compositions, thermal, optical and structural properties was further studied according to two specific series of glasses labelled (i) “BaO” (marked with \blacklozenge in Figure 1) and (ii) “GeO₂” (marked with \blacktriangleright in Figure 1). The first series has been designed to investigate the influence of the barium oxide content while keeping fixed the ratios $\text{GaO}_{3/2} : \text{GeO}_2 (= 1:2)$ and $\text{LaO}_{3/2} : \text{GaO}_{3/2} (= 4:5)$. The first ratio has been fixed to maintain the proportion of network glass former and the second ratio assumes that equivalent amount of lanthanum and gallium ensure the compensation of the $(\text{GaO}_4)^-$ units. The second series focus on the influence of the germanium oxide content while preserving the ratios $\text{LaO}_{3/2} : \text{GaO}_{3/2} (= 4:1)$ for a fixed barium oxide content equals to 10 cationic molar percent. We summarized the investigated glass compositions in Table 1. Beside the composition corresponding to Ge-0, all compositions corresponding to the glassy domain have been reproduced for the study using classical melt quench techniques in platinum crucible.

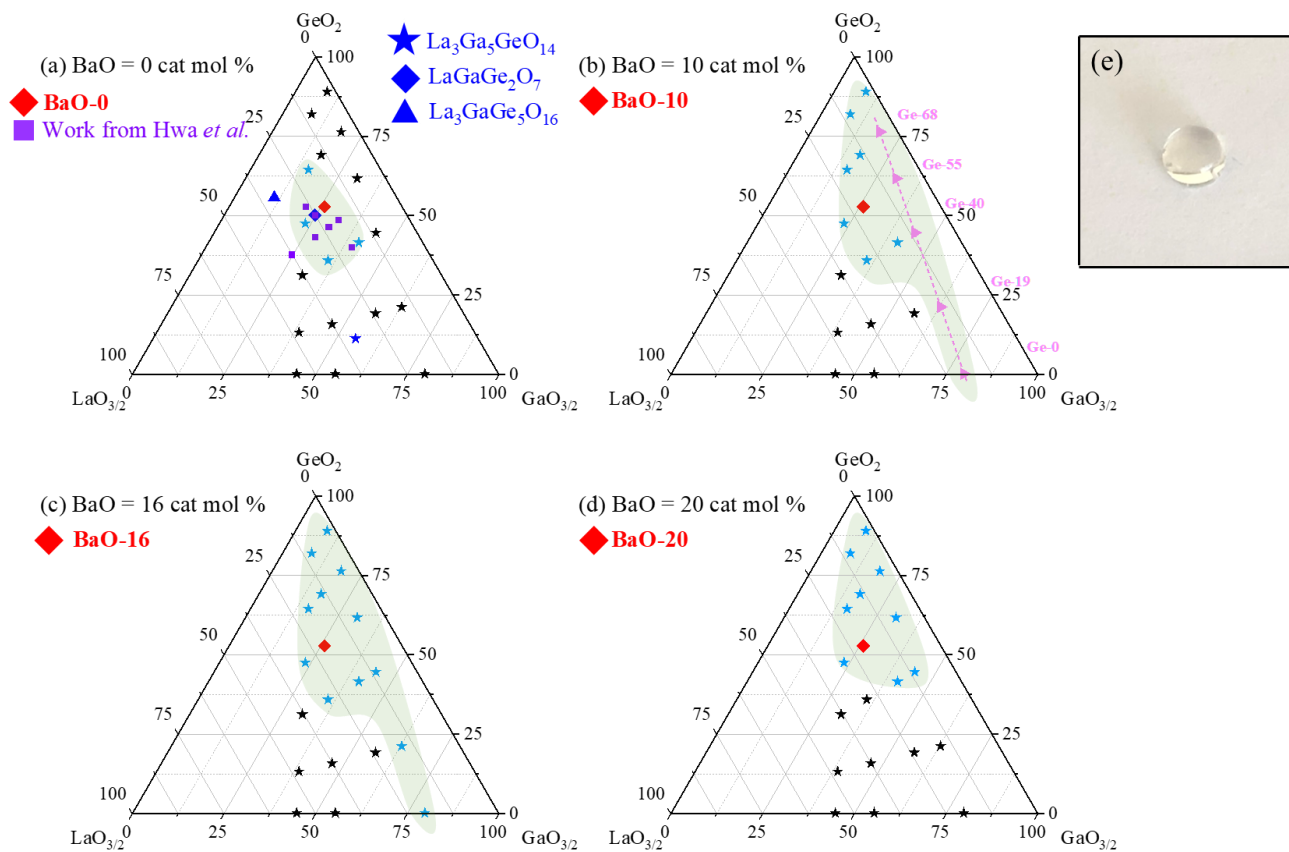


Figure 1: Glass forming multicomponent vitreous formation diagrams in the pseudo-ternary system $(1 - \alpha) (x \text{ GaO}_{3/2} - y \text{ GeO}_2 - z \text{ LaO}_{3/2}) - \alpha \text{ BaO}$ varying the barium oxide content α as follows: (a) 0 (b) 10 (c) 16 (d) 20 cationic molar percent (abbreviated cat mol %). The obtained vitreous formation domains are highlighted with “ \bullet ”. This mark should be considered as a guide for eyes, “ \star ”: crystalline state, “ \star ”: glassy state, “ \blacklozenge ”: investigated samples in the BaO series, “ \blacktriangle ”: investigated samples in the GeO_2 series, “ $\star\star\blacklozenge$ ”: main crystalline phases, “ \blacksquare ”: work reported by Hwa *et al.* [30]. Picture of one obtained glass samples is shown in (e).

		Compositions (mol %)				Compositions (cat mol %)				Cationic molar ratios (cat mol %)	
Sample		Ga_2O_3	GeO_2	La_2O_3	BaO	$\text{GaO}_{3/2}$	GeO_2	$\text{LaO}_{3/2}$	BaO	$R = \text{GaO}_{3/2} : \text{GeO}_2$	$Q = (2\text{BaO} + 3\text{LaO}_{3/2}) : \text{GaO}_{3/2}$
\blacklozenge BaO glass series	BaO-0	17.24	68.97	13.79	0.00	26.32	52.63	21.05	0.00	0.5	2.40
	BaO-10	15.00	60.00	12.00	13.00	23.62	47.24	18.90	10.24	0.5	3.27
	BaO-16	13.71	54.84	10.97	20.48	21.99	43.98	17.60	16.43	0.5	3.89
	BaO-20	12.99	51.95	10.38	24.68	21.06	42.11	16.83	20.00	0.5	4.30
\blacktriangle GeO_2 glass series	Ge-0	65.14	0.00	16.28	18.58	71.81	0.00	17.95	10.24	-	1.04
	Ge-19	43.90	29.27	10.97	15.86	56.69	18.90	14.17	10.24	3	1.11
	Ge-40	26.57	53.14	6.65	13.64	39.89	39.89	9.98	10.24	1	1.26
	Ge-55	16.69	66.76	4.17	12.38	27.62	55.24	6.90	10.24	0.5	1.49
	Ge-68	9.57	76.57	2.39	11.47	17.10	68.39	4.27	10.24	0.25	1.95

Table 1: Selected glass series and their theoretical compositions in the glass forming pseudo-ternary diagrams $\text{GaO}_{3/2} - \text{GeO}_2 - \text{LaO}_{3/2} - \text{BaO}$ (molar percentage and cationic molar percentage) – Main theoretical cationic ratios has been defined as $R = \text{GaO}_{3/2} : \text{GeO}_2$ and $Q = (2\text{BaO} + 3\text{LaO}_{3/2}) : \text{GaO}_{3/2}$.

Table 2: Thermal properties (T_g : onset of the glass transition temperature; T_x : onset of the crystallization temperature and ΔT : thermal stability ($T_x - T_g$)) and physical properties (ρ : bulk density) of the investigated glass samples.

	Sample	T_g (± 4 °C)	T_x (± 4 °C)	ΔT (± 8 °C)	ρ (± 0.01 g.cm ⁻³)
◆ BaO glass series	BaO-0	728	837	109	5.20
	BaO-10	718	843	125	5.14
	BaO-16	714	863	149	5.10
	BaO-20	713	841	128	4.91
► GeO₂ glass series	Ge-0	748	825	77	5.39
	Ge-19	718	826	108	5.18
	Ge-40	713	857	144	4.97
	Ge-55	661	810	149	4.67
	Ge-68	639	728	89	4.43

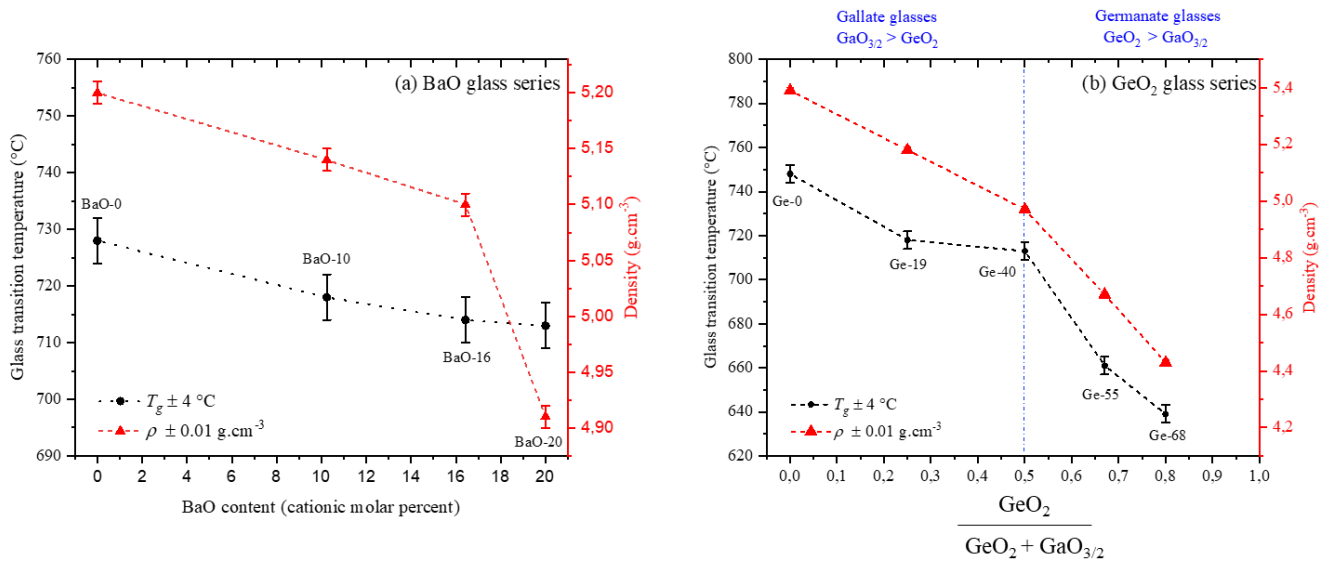


Figure 2: Glass transition temperatures T_g and bulk densities versus their respective (a) barium oxide BaO and (b) the $\text{GeO}_2 / (\text{GeO}_2 + \text{GaO}_{3/2})$ ratio. The dashed lines are guides for eyes. The blue dashed line denotes the separation between germanate ($\text{GaO}_{3/2} < \text{GeO}_2$) and gallate ($\text{GaO}_{3/2} > \text{GeO}_2$) compositions.

Physical and thermal properties.

The glass transition temperature, the onset temperature of the crystallization and the “thermal stability” toward crystallization $\Delta T (= T_x - T_g)$ and the glass density for both glass series are reported in Table 2.

Regarding the BaO glass series, as depicted in Figure 2a, both the glass transition temperature and the density evolve nonlinearly versus the barium oxide content. The introduction of BaO is first characterized by

a linear decrease of the glass density from $5.20 \pm 0.01 \text{ g.cm}^{-3}$ down to $5.10 \pm 0.01 \text{ g.cm}^{-3}$ between BaO-0 and BaO-16 samples respectively and then drop for cationic mol% of BaO above 16. The glass transition temperatures T_g decrease continuously from 728 °C for BaO-0 down to 714 °C for BaO-16 samples. Then, glass transition T_g appears fairly constant for BaO-16 and BaO-20. The decrease of the glass transition temperature can be related to the lowest Ba – O bond dissociation energy ($D_{298K}^0 = 562 \text{ kJ/mol}$ [35]) as compared to La – O ($D_{298K}^0 = 798 \text{ kJ/mol}$ [35]) and also to the fact that the proportion of germano-gallate glass skeleton decreases when the barium oxide content increases. However, the nonlinear evolution of the glass transition temperature and the density versus the barium oxide concentration indicates a structural change between the BaO-0 to the BaO-16 composition which becomes important above 16 cationic molar % of BaO.

Regarding the GeO_2 glass series, the evolution of the physical properties of the GeO_2 series seems to follow two different behaviors which are related to the proportion of the main glass former constituent, *i.e.* germanate ($\text{GaO}_{3/2} / \text{GeO}_2 < 1$) or gallate ($\text{GaO}_{3/2} / \text{GeO}_2 > 1$). The two domains are separated by the blue dashed line in Figure 2b. The strongest rate corresponds to the germanate network part (Ge-68 to Ge-40) and the slowest for gallate glasses (Ge-40 to Ge-0). Indeed, an important density change from $4.43 \pm 0.01 \text{ g.cm}^{-3}$ up to 4.97 g.cm^{-3} occurs between the germanate samples labelled Ge-68, Ge-55 and Ge-40. A strong change of the glass transition temperatures from 639 °C up to 713 °C (+74 °C) can be also observed for the samples Ge-68 and Ge-40 respectively. In this series, a threshold appears around $\text{GaO}_{3/2} : \text{GeO}_2 \sim 1$ which corresponds to the Ge-40 sample. In the gallate glass domain, the glass transition temperatures evolve slightly from 713 °C up to 748 °C (+35 °C) for the sample Ge-40 and Ge-0 respectively. One has to remember that in this last composition range, the amount of $\text{GaO}_{3/2}$ increases faster only from 39.89 cat mol % up to 71.81 cat mol %. The T_g evolution is most probably mainly related to the change of the network glass former even if the lanthanum oxide content increases also in this composition range. Regarding the density, the evolution versus the proportion of germanium is less pronounced than for the glass transition temperature. Nevertheless, a decrease of the slope of the density evolution versus the germanium oxide proportion in the gallate glass section when $\text{GeO}_2 < \text{GaO}_{3/2}$ can be observed in Figure 2b.

Optical Transmission

The transmission spectra for the BaO and GeO_2 glass series shown in Figure 3 display a large transmission window ranging from ultraviolet λ_{UV} (~ 300 nm) up to mid-infrared λ_{IR} (~ 5 500 nm). A large asymmetric broad band ranging from ~ 2700 nm up to ~ 3600 nm can be assigned to the stretching vibrations of hydroxyl ions which is related to the absence of specific purification steps during the glass synthesis. The absorption band around ~ 4 200 nm could be assigned to the overtone of a stretching motion such as Ge – OH. Regarding the infrared cut-off, notable spectral variations can be seen in Figure 3b depending on the amount of barium oxide content. The cut-off at the lowest wavelength seems to be related to a strong absorption band located around ~ 6 200 nm for the BaO-20 sample. Several structural aspects affecting the infrared vibrations and their overtone have to be taken into account for assigning this spectral change, making a clear correlation difficult.

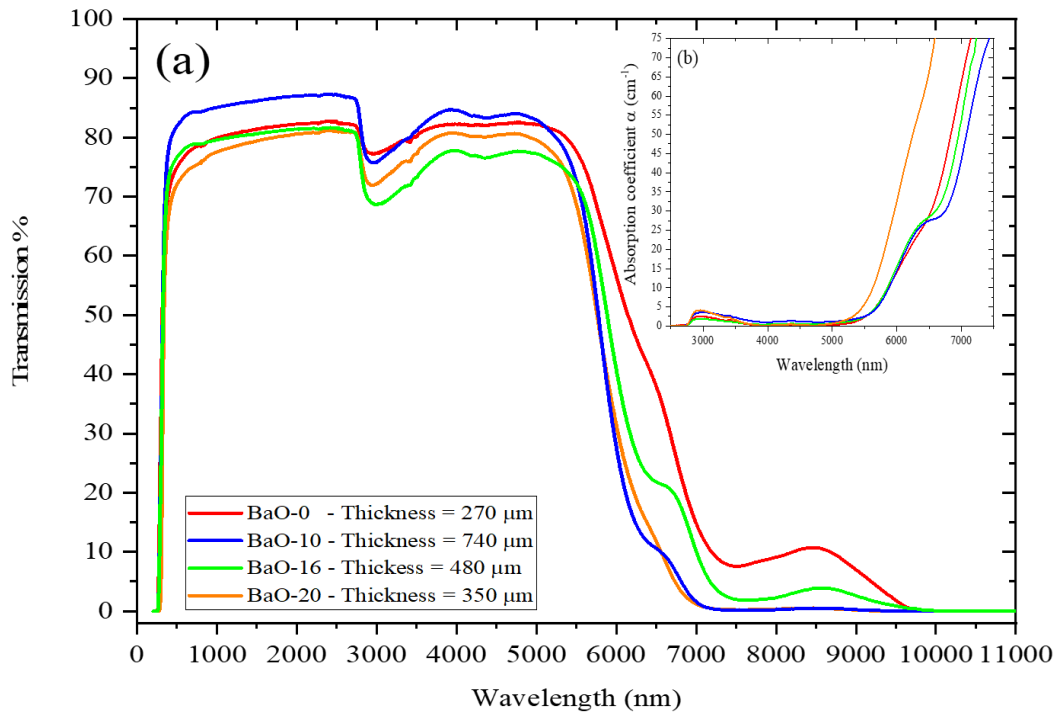


Figure 3: (a) Transmission spectra of the BaO glass series and their respective thickness - Absorption coefficient calculated in (b) the near-and mid-infrared range for the BaO-0, BaO-10, BaO-16 and BaO-20 glass samples.

In the GeO_2 glass series, the insertion of gallium oxide in the germanate networks contributes to extend the infrared transparency from $\sim 5\,500$ nm to $\sim 6\,500$ nm as depicted in Figure 4a. The infrared cut-off is mainly related to the presence of an absorption band around 6200 nm and 7200 nm which is well seen on the richest GeO_2 containing sample (Ge-68) sample (Figure 4b). This latter sample was polished down to a thin thickness lower than $200\ \mu\text{m}$ allowing to visualize the band maximum position by transmission measurement. One can also notice that the absorption band located between 2700 nm and 3600 nm previously assigned to hydroxyl ions disappear for the pure gallate sample Ge-0. This suggests that the hydroxyl group presence is related to the introduction of germanium oxide in the glass composition.

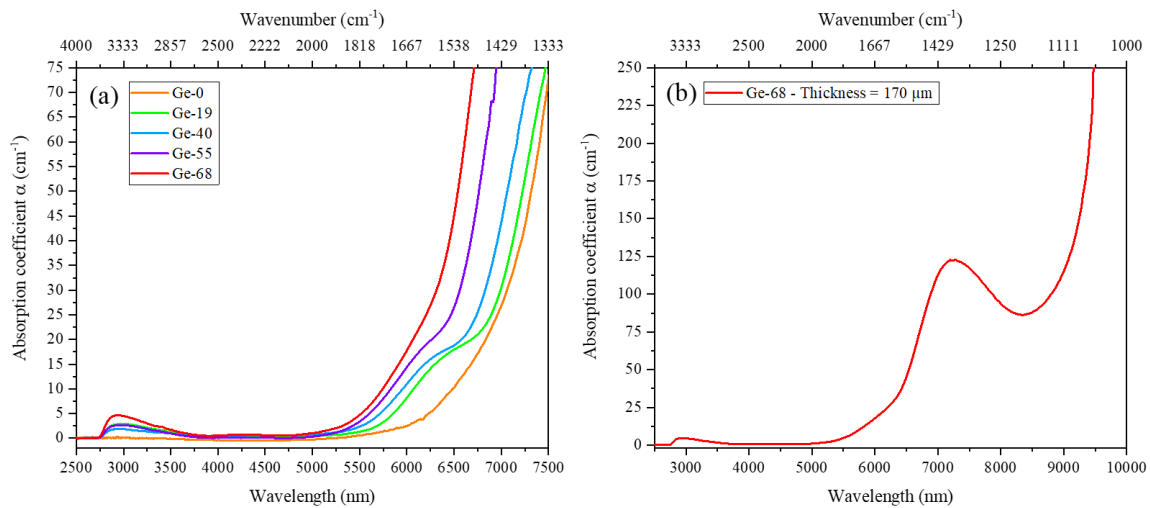


Figure 4: (a) Absorption coefficient for the GeO₂ series – (b) Absorption coefficient for a thin polished glass sample Ge-68 (thickness = 170 μm)

Vibrational spectroscopy analysis

Unpolarized Raman and Fourier transformed infrared spectra from BaO and GeO₂ investigated series are respectively presented in Figure 5 and in Figure 6. The spectra have been normalized to the broad band located around 500 cm⁻¹. Regarding the BaO-16 and Ge-19 compositions, the small size of the sample obtained did not allow recording FTIR spectra. Those vibrational spectra exhibit two main contributions in low and high frequency regions respectively located between 400 – 630 cm⁻¹ and 630 – 1000 cm⁻¹. The lowermost frequency region is mainly characteristic to a combination of stretching $\nu(T^{[4]} - O - T^{[4]})$ and $\delta(T^{[4]} - O - T^{[4]})$ bending modes of an oxygen surrounded by two tetrahedral units (T = gallium, germanium) linked by their corners [36]. The uppermost domain are reported to contain more localized stretching features of germanium and gallium sites involved respectively in $Q_n = 1,2,3,4$ germanate units [37] and Q_4 gallate units [29], [34] [36]. As previously reported, Raman active vibrations in this frequency domains involve germanium tetrahedra with non-bridging oxygens [36], [38], but stretching vibrations from $T^{[4]} - O - T^{[4]}$ skeleton in a mixed interconnected $Ga^{[4]} - O - Ge^{[4]}$ bridges are also expected [36]. While these stretching vibrations are inactive in Raman in Ge – O – Ge bridges, the presence of an additional negative electronic contribution on the oxygen along the mixed interconnected $Ga^{[4]} - O - Ge^{[4]}$ bridges make those vibrational modes both Raman and IR active [36]. The negative charge on oxygen ions is, in this case, balanced by the barium or lanthanum cation.

In the BaO series, regarding the low frequency band, two main spectral variations can be highlighted upon the insertion of barium oxide: (i) a shrink of the Raman band between 400 and 600 cm⁻¹ and (ii) a shift of the maximum intensity from ~ 530 cm⁻¹ down to ~ 510 cm⁻¹. The Raman peak around ~ 530 cm⁻¹ has already been reported by several authors [26], [36] and assigned to coupled bending and stretching vibrational modes of Ga – O – Ge bridges in which positive cations act as charge compensator and in which (Ga, Ge) tetrahedra are connected with their corners. The shift to lower frequency could indicate a depolymerization of the glass skeleton upon the increase of the barium oxide content. In the high frequency region above 650 cm⁻¹, in order

to illustrate the evolution, the Raman and infrared spectra have been deconvoluted in the high frequency region for the BaO series using five vibration contributions located at $\sim 690 \text{ cm}^{-1}$ (labelled “1”), $\sim 755 \text{ cm}^{-1}$ (labelled “2”), $\sim 785 \text{ cm}^{-1}$ (labelled “3”), $\sim 825 \text{ cm}^{-1}$ (labelled “4”) and 890 cm^{-1} (labelled “5”). Gaussian mathematical functions have been selected for the simulation. For the simulation of the various compositions, the Raman and infrared spectra have been deconvoluted using Gaussian function with “*quasi-identical*” wavenumber positions (variation of the peaks position maintained below 15 cm^{-1}) and constant width. To take into account the low frequency region contribution on the high frequency region, a unique vibration has been implemented in order to simulate the tail effect. The vibrational band wavenumber and assignments used for the deconvolution from both series are respectively listed in Table 3. Based on the work of Kamitsos *et al.* [39] on Germanium – Rubidium glass systems, the bands located around $\sim 755 \text{ cm}^{-1}$ (# 2) and $\sim 825 \text{ cm}^{-1}$ (# 4) can be respectively attributed to $\nu(\text{Ge} - \text{O})$ stretching vibration respectively in $Q_2(\text{GeO}_2\text{O}_2)$ or Q_3 units (GeO_3O^-) respectively. Following the work from Skopak *et al.* [36] the Raman and infrared bands positioned around $\sim 785 \text{ cm}^{-1}$ (# 3) and $\sim 890 \text{ cm}^{-1}$ (# 5) can be ascribed to localized stretching vibrational modes involved in $\text{T}^{[4]} - \text{O} - \text{T}^{[4]}$ bridges. The combined Raman and infrared activity indicates the presence of negatively charged $\text{Ge}^{[4]} - \text{O}^- - \text{Ga}^{[4]}$ bonds with alternatively interconnected gallium and germanium tetrahedra where the charge compensation of those links is either achieved by lanthanum or barium cations. The remaining vibrational modes located at $\sim 690 \text{ cm}^{-1}$ (# 1) could be assigned to localized stretching frequency $\nu(\text{Ga} - \text{O})$ in $Q_3(\text{GaO}_4)^{2-}$ units being charge compensated with either barium or lanthanum as proposed by Yoshimoto *et al.* [40]. In relative intensity, the intensities of the bands located around $\sim 755 \text{ cm}^{-1}$ (# 2) and $\sim 825 \text{ cm}^{-1}$ (# 4) increases significantly while raising the BaO content. Even if Kamitsos *et al.* [39] attributed those vibrations to Q_2 and Q_3 units, one has to be prudent here on a precise assignment in particular on the band at 755 cm^{-1} . Nevertheless, it remains reasonable to claim that the evolution of those vibrations correspond to the presence on non-bridging oxygen on germanium moieties. Further structural characterizations such as ^{71}Ga NMR need to be performed for a more detailed assignment.

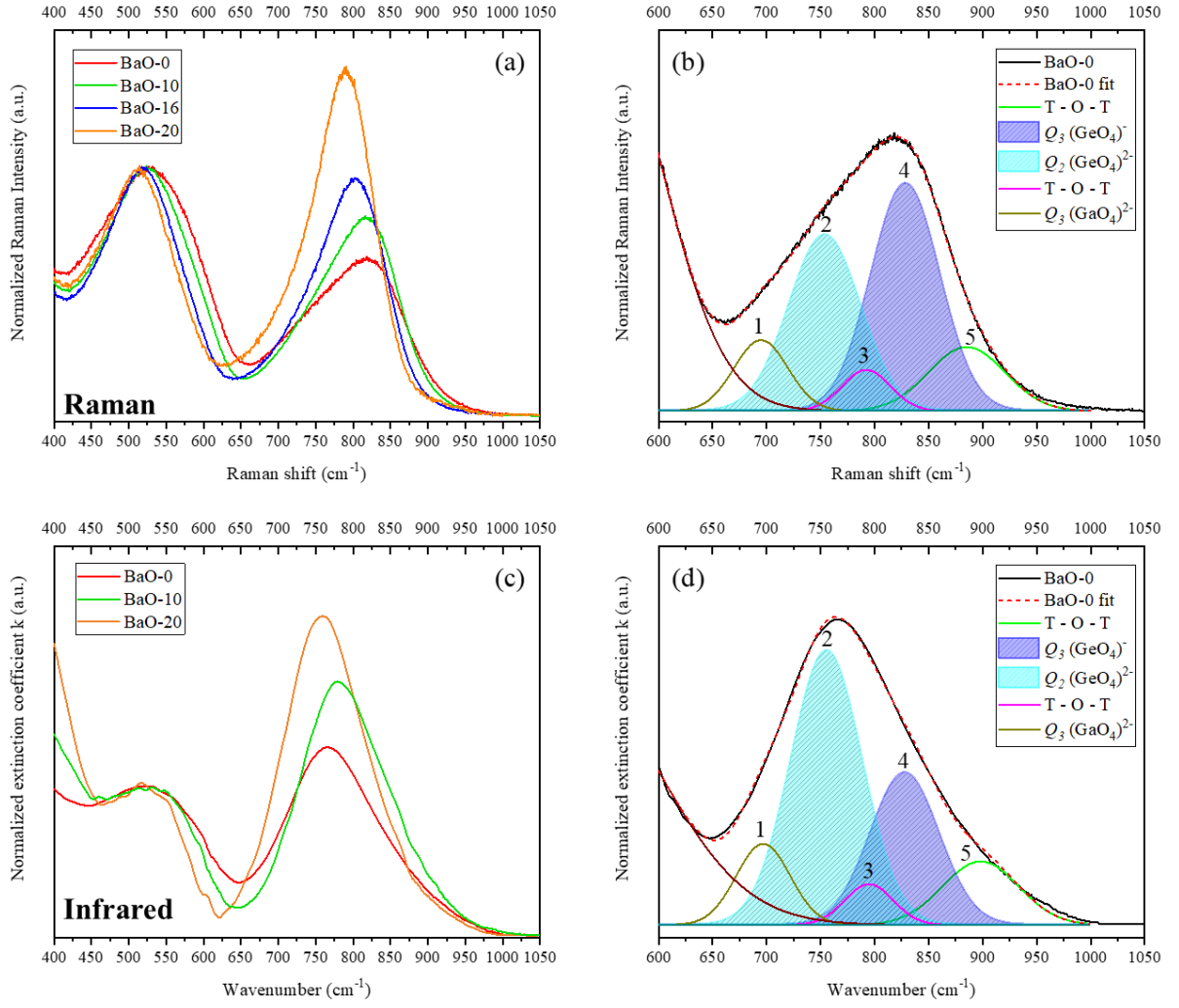


Figure 5: (a) Unpolarized Raman spectra for the BaO series and (b) Raman deconvoluted spectra for the glass sample BaO-0 (c) Fourier transformed infrared spectra for the BaO series. (c) Fourier transformed infrared spectra deconvoluted for the glass sample BaO-0 for the high wavenumber frequency section fitting the tail of the low frequency region are fitted with a single Gaussian.

Band number	Wavenumber (cm ⁻¹)	Assignments	References
1	~ 690	ν (Ga - O) stretching involved in Q_3 (GaO ₄) ⁻ units being charge compensated	[33]
2	~ 755	ν (Ge - O) stretching involved in Q_2 units (GeO ₂ O ₂) ²⁻	[39]
3	~ 785	ν (T ^[4] - O - T ^[4]) including mainly Ga - O - Ge alternance	[34]
4	~ 825	ν (Ge - O) stretching involved in Q_3 units (GeO ₃ O) ⁻	[39]
5	~ 890	ν (T ^[4] - O - T ^[4]) including mainly Ga - O - Ge alternance	[34]

Table 3: Main Raman and infrared vibrational modes representing the high frequency region in the investigated BaO glass series based on the literature

The Raman and infrared spectra of the GeO_2 glass series with $\text{LaO}_{3/2}/\text{GaO}_{3/2}$ constant ratio, are presented in Figure 6. In the low frequency region, the Raman peak shifts from $\sim 510 \text{ cm}^{-1}$ up to 530 cm^{-1} while the Infrared peak shifts from $\sim 554 \text{ cm}^{-1}$ down to $\sim 502 \text{ cm}^{-1}$. Those shifts are assigned to the vibrational spectral signatures of a change of network skeleton from $\text{Ge} - \text{O} - \text{Ge}$ combined vibrational modes for the benefit $\text{Ga} - \text{O} - \text{Ge}$ bridges while adding gallium oxide. In the high frequency region, the band located above 800 cm^{-1} previously ascribed to $\text{T} - \text{O} - \text{T}$ bridges alternating germanium and gallium tetrahedral and Q_3 germanate units is no more present in the pure gallate glass matrix in Raman and Infrared spectroscopy. This effect is clearly visible in the infrared spectra showing that the asymmetric stretching of germanium units with non-bridging oxygens vibrating above 800 cm^{-1} decreases in magnitude when the germanium oxide content decreases and shifts from 825 cm^{-1} for Ge-68 to reach 760 cm^{-1} for the composition Ge-40. In the case of pure gallate sample (Ge-0), the contribution around $\sim 760 \text{ cm}^{-1}$ could be related to $\nu(\text{Ga}-\text{O}-\text{Ga})$ stretching mode [41], [42]. In this gallate glass composition, new contributions are observed around $\sim 630 \text{ cm}^{-1}$ and $\sim 690 \text{ cm}^{-1}$ in the Raman and IR spectra respectively which increases upon the addition of gallium oxide content. Yoshimoto *et al.* in binary lanthanum-gallate glasses have assigned the Raman band at around 630 cm^{-1} to $\nu(\text{Ga}^{[4,5,6]} - \text{O})$ stretching vibration arising from either gallium polyhedra $(\text{GaO}_x)_{4 \leq x \leq 6}$ with possibly non-bridging oxygens (NBOs) or gallate tri-clusters $(\text{Ga}^{[4]} - \text{O}^{[3]})$ [41].

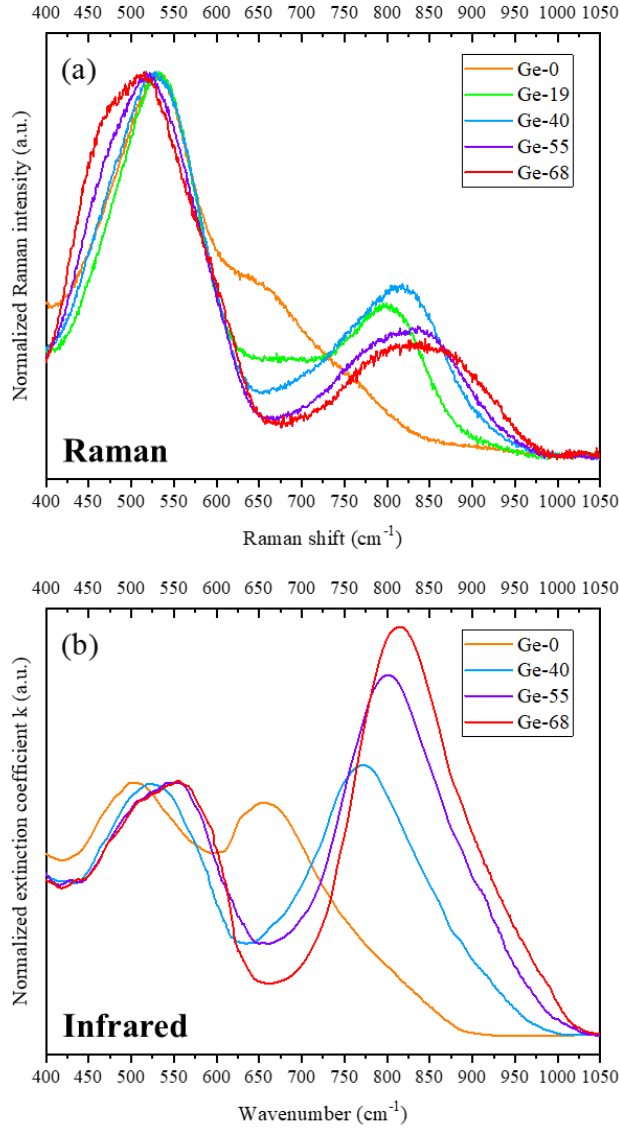


Figure 6: (a) Unpolarized Raman spectra and (b) Fourier Transformed InfraRed spectra for the GeO₂ glass series

Discussion.

The key points for understanding the germano – gallate glass structures and properties rely on the investigation of the charge compensation mechanism of charged gallate units, in particular the [GaO₄]⁻ units and the formation of either by $Q_i = 1, 2, 3, 4$ germanate or gallate units. The glass structure can be compared to the aluminosilicate glass structures. Indeed, gallium cations are expected to act as aluminum in (M₂O or MO) – Al₂O₃ – SiO₂ –based vitreous systems [21], [38]. In other words, gallium oxide, as alumina oxide, generally enters into the network in four-fold tetrahedral corner shared entities. Once inserted, Ga³⁺ (Al³⁺) substitute Ge⁴⁺ (Si⁴⁺) which produces an additional localized negative charge on the Ga^[4] (Al^[4]) – O⁻ – Ge^[4] (Si^[4]) bridges. Those links are then charge-balanced by M^{z+} cations, acting mostly as charge compensators. At this point, both cases could be considered depending on the polymerization and the charge ratios respectively defined as $R = [\text{GaO}_{3/2}] / [\text{GeO}_2]$ and $Q = z^+ [\text{M}] / [\text{GaO}_{3/2}]$. When $R > 1$ and $Q \leq 1$, gallate units tend to change

their coordination number, forming a fraction of higher coordinated gallate units such as GaO_5 or GaO_6 [36]. Whereas R and Q fulfill the conditions $R \leq 1$ and $Q \geq 1$, the remaining M^{z+} positive cations depolymerizes the network, acting as glass modifiers [36]. Those cations create mainly localized non-bridging oxygens (labelled “NBOs”) on germanate tetrahedra with localized stretching at 755 cm^{-1} and 825 cm^{-1} units. The investigated barium series (BaO) fully satisfy the conditions $R \leq 1$ and $Q \geq 1$. In agreement with both Infrared and Raman vibrational activity assigned to $\text{T}^{[4]} - \text{O} - \text{T}^{[4]}$ stretching modes, the glass skeleton is made of a three-dimensional corner shared tetrahedral formed with $\text{Ga}^{[4]} - \text{O} - \text{Ge}^{[4]}$ bridges. The gallium lies in tetrahedral sites and its charge compensation is mainly satisfied by lanthanum La^{3+} or barium Ba^{2+} cations. For $Q \geq 1$, the excess of positive charges produces mainly non-bridging oxygens on germanium sites $Q_3 (\text{GeO}_3\text{O})^-$. Indeed, the Raman vibration localized at 755 cm^{-1} corresponding to NBOs on germanate entities becomes dominant above 16 cat mol % of BaO.

Regarding the structure – properties relationships, the slight decrease of the density upon the barium oxide insertion up to 16 cat mol % follows the glass structure evolution with the progressive appearance of germanium site with non-bridging oxygen which tend to depolymerize the glass skeleton formed of corner shared tetrahedra. For BaO-20 glass, for which the NBOs vibration becomes predominant, a significant density drop can be observed. This evolution of the density is accompanied by a continuous decrease of the glass transition temperature which tend to stabilize for BaO-16 and BaO-20. This evolution is again in accordance with the progressive depolymerization of the glass network.

Regarding the GeO_2 glass series, the composition range investigated covers two different glass networks: (i) germanate-based glass network from Ge-68 to Ge-40 and (ii) gallate-based network from Ge-40 up to Ge-0. In Figure. 2, two different evolutions for the glass transition temperatures and the densities are clearly observed depending on the main network former. Regarding the germanate part (Ge-68 to Ge-40), the glass network polymerizes with the progressive increase of gallium oxide, leading to the formation of $\text{Ge} - \text{O} - \text{Ga}$ bridges in which the gallium tetrahedra are charged-balanced by lanthanum and barium. This structural evolution is in accordance with the linear increase of T_g and densities. Above Ge-40, the slope of T_g and density versus the amount of $\text{GaO}_{3/2}$ evolves slowly. This evolution corresponds to the disappearance of the germanium sites with non-bridging oxygens and the formation of a gallate glass network. Those physical variations may rely on the formation of new polyhedral units such as $(\text{GaO}_x)_{4 \leq x \leq 6}$ units with possible non-bridging oxygens or oxygen tri-clusters ($\text{Ga} - \text{O}^{[3]}$). Nonetheless, such hypothesis needs to be confirmed by ^{17}O NMR for instance.

Conclusion

The existence domains of glass in the multicomponent $\text{GaO}_{3/2} - \text{GeO}_2 - \text{LaO}_{3/2} - \text{BaO}$ pseudo-ternary diagrams while varying the amount of Barium oxide from 0 cat mol % up to 20 cat mol % were determined using aerodynamic levitation coupled to laser heating as a synthesis tool. The introduction of barium oxide allows the glass-forming region to be widened. Gallium and germanium ions occupy tetrahedral sites and form a three dimensional network with T-O-T bridges (T = Ge, Ga). In germano-gallate glass network, the barium and lanthanum ions play the role of charge compensator of oxygen in Ge-O-Ga bridges. The excess of positive charge is mainly balanced by the formation of $Q_3 (\text{GeO}_3\text{O})^-$ germanate units. The decrease of the glass

transition temperatures is associated with the progressive increase of those Q₃ units on the germanium. The extended infrared transmission of gallate is proposed to be related with the existence of gallium oxygenated sites with possibly non-bridging oxygens or the formation of oxygen tri-clusters vibrating at lower frequency than that of germanium germano-gallate based structural units.

Acknowledgements

This research was supported by Agence Nationale de la Recherche (ANR) (ANR-18-CE08-0004-02) and the New Aquitaine Region. This project has received funding from the European Union's Horizon 2020 research and innovation program under the Marie Skłodowska-Curie grant agreement No 823941 (FUNGLASS), as well as grants of the Agence Nationale de la Recherche (ANR) with the program "Investissement d'avenir" number ANR-10-IDEX-03-02. M. Nalin acknowledges the São Paulo Research Foundation, FAPESP (grant numbers 2013/07793-6 and 2019/01223-0). The authors acknowledge the platform SIV for vibrational spectroscopy characterizations.

References

- [1] M. Sieger et B. Mizaikoff, "Toward On-Chip Mid-Infrared Sensors", *Anal. Chem.*, vol. 88, n° 11, p. 5562-5573, juin 2016, doi: 10.1021/acs.analchem.5b04143.
- [2] N. A. Diakides et J. D. Bronzino, "*Medical Infrared Imaging*". CRC Press, 2007.
- [3] W. H. Dumbaugh et J. C. Lapp, "Heavy-Metal Oxide Glasses", *J American Ceramic Society*, vol. 75, n° 9, p. 2315-2326, sept. 1992, doi: 10.1111/j.1151-2916.1992.tb05581.x.
- [4] W. H. Dumbaugh, "Oxide Glasses With Superior Infrared Transmission", in *Advances in Optical Materials*, déc. 1984, vol. 0505, p. 97-101, doi: 10.1117/12.964633.
- [5] S. J. L. Ribeiro, J. Dexpert-Ghys, B. Piriou, et V. R. Mastelaro, "Structural studies in lead germanate glasses: EXAFS and vibrational spectroscopy", *Journal of Non-Crystalline Solids*, vol. 159, n° 3, p. 213-221, janv. 1993, doi: 10.1016/0022-3093(93)90225-M.
- [6] Fumiaki Miyaji, Sumio Sakka, "Structure of PbO-Bi₂O₃-Ga₂O₃ glasses," *Journal of Non-Crystalline Solids*, Volume 134, Issues 1–2, 1991, Pages 77-85, ISSN 0022-3093, [https://doi.org/10.1016/0022-3093\(91\)90013-V](https://doi.org/10.1016/0022-3093(91)90013-V).
- [7] B. G. Aitken and N. F. Borelli, "Thallium gallate glasses," US 5,168,079, 1992.
- [8] N. F. Borrelli, H. Dumbaugh, D. W. Hall, M. A. Newhouse, M. L. Powley, et D. L. Weidman, « galliobismuthate gallate glasses », US 5,093,287
- [9] J. C. Lapp and M. L. Powley, "Alkali bismuth gallate glasses," US 5,114,884, 1992.
- [10] Fumiaki Miyaji, Kiyoharu Tadanaga, Toshinobu Yoko, Sumio Sakka, "Coordination of Ga³⁺ ions in PbO-Ga₂O₃ glasses as determined by ⁷¹Ga NMR", *Journal of Non-Crystalline Solids*, Volume 139, 1992, Pages 268-270, ISSN 0022-3093, [https://doi.org/10.1016/S0022-3093\(05\)80834-8](https://doi.org/10.1016/S0022-3093(05)80834-8).
- [11] John M. Jewell, Jacqueline A. Ruller, "A structural model for PbO-Ga₂O₃-SiO₂ glasses", *Journal of Non-Crystalline Solids*, Volume 152, Issues 2–3, 1993, Pages 179-187, ISSN 0022-3093, [https://doi.org/10.1016/0022-3093\(93\)90249-W](https://doi.org/10.1016/0022-3093(93)90249-W).
- [12] J. Yumoto, S. G. Lee, B. Kippelen, N. Peyghambarian, B. G. Aitken, et N. F. Borrelli, "Enhancement of optical nonlinearity of heavy-metal oxide glasses by replacing lead and bismuth with thallium", *Appl. Phys. Lett.*, vol. 63, n° 19, p. 2630-2632, nov. 1993, doi: 10.1063/1.110403.
- [13] H. Lin, L. W. Dechent, D. E. Day, et J. O. Stoffer, "IR transmission and corrosion of lead-bismuth gallate glasses", *Journal of Non-Crystalline Solids*, vol. 171, n° 3, p. 299-303, août 1994, doi: 10.1016/0022-3093(94)90199-6.
- [14] J. A. Ruller et J. M. Jewell, "Raman and infrared spectra of lead gallosilicate glasses", *Journal of Non-Crystalline Solids*, vol. 175, n° 1, p. 91-97, sept. 1994, doi: 10.1016/0022-3093(94)90319-0.
- [15] J. Heo, Y. B. Shin, et J. N. Jang, "Spectroscopic analysis of Tm³⁺ in PbO-Bi₂O₃-Ga₂O₃ glass", *Appl. Opt.*, vol. 34, n° 21, p. 4284, juill. 1995, doi: 10.1364/AO.34.004284.
- [16] A. C. Hannon, J. M. Parker, et B. Vessal, "The effect of composition in lead gallate glasses: a structural study", *Journal of Non-Crystalline Solids*, vol. 196, p. 187-192, mars 1996, doi: 10.1016/0022-3093(95)00584-6.

- [17] A. A. Kharlamov, R. M. Almeida, et J. Heo, "Vibrational spectra and structure of heavy metal oxide glasses", *Journal of Non-Crystalline Solids*, vol. 202, n° 3, p. 233-240, juill. 1996, doi: 10.1016/0022-3093(96)00192-5.
- [18] Y. G. Choi, J. Heo, et V. A. Chernov, "Ga K-edge EXAFS analysis on the coordination of gallium in PbO–Ga₂O₃ glasses", *Journal of Non-Crystalline Solids*, vol. 221, n° 2-3, p. 199-207, déc. 1997, doi: 10.1016/S0022-3093(97)00418-3.
- [19] D. Lezal, J. Pedlikova, P. Kostka, J. Bludska, M. Poulain, et J. Zavadil, "Heavy metal oxide glasses: preparation and physical properties", *Journal of Non-Crystalline Solids*, vol. 284, n° 1-3, p. 288-295, mai 2001, doi: 10.1016/S0022-3093(01)00425-2.
- [20] S. Simon et V. Simon, "Thermal characterisation of gallium-bismuthate oxide glasses", *Materials Letters*, vol. 58, n° 29, p. 3778-3781, nov. 2004, doi: 10.1016/j.matlet.2004.07.042.
- [21] P. L. Higby et I. D. Aggarwal, "Properties of barium gallium germanate glasses", *Journal of Non-Crystalline Solids*, vol. 163, n° 3, p. 303-308, déc. 1993, doi: 10.1016/0022-3093(93)91308-P.
- [22] S. S. Bayya, B. B. Harbison, J. S. Sanghera, et I. D. Aggarwal, "BaO-Ga₂O₃-GeO₂ glasses with enhanced properties", *Journal of Non-Crystalline Solids*, vol. 212, n° 2, p. 198-207, juin 1997, doi: 10.1016/S0022-3093(96)00658-8.
- [23] S. S. Bayya, G. D. Chin, J. S. Sanghera, et I. D. Aggarwal, "Germanate glass as a window for high energy laser systems", *Optics Express*, vol. 14, n° 24, p. 11687, 2006, doi: 10.1364/OE.14.011687.
- [24] S. S. Bayya, G. D. Chin, G. Villalobos, J. S. Sanghera, et I. D. Aggarwal, "VIS-IR transmitting windows", Orlando, Florida, USA, mai 2005, p. 262, doi: 10.1117/12.603753.
- [25] I. S. S.- Bayya, J. S. Sanghera, et I. D. Aggarwal, "Optical transmission of BGG glass material", WO 2005069761 A2, 2004.
- [26] T. Skopak, F. Calzavara, Y. Ledemi, F. Célarié, M. Allix, E. Véron, M. Dussauze, T. Cardinal, E. Fargin, Y. Messaddeq, "Properties, structure and crystallization study of germano-gallate glasses in the Ga₂O₃-GeO₂-BaO-K₂O system", *Journal of Non-Crystalline Solids*, vol. 514, p. 98-107, juin 2019, doi: 10.1016/j.jnoncrysol.2019.02.028.
- [27] T. Guérineau, C. Strutynski, T. Skopak, S. Morency, A. Hanafi, F. Calzavara, Y. Ledemi, S. Danto, T. Cardinal, Y. Messaddeq, E Fargin, "Extended germano-gallate fiber drawing domain: from germanates to gallates optical fibers", *Opt. Mater. Express*, vol. 9, n° 6, p. 2437, juin 2019, doi: 10.1364/OME.9.002437.
- [28] S. Szu, C. Shu, et L.-G. Hwa, « Structure and properties of lanthanum gallio germanate glasses », *Journal of Non-Crystalline Solids*, vol. 240, n° 1-3, p. 22-28, oct. 1998, doi: 10.1016/S0022-3093(98)00710-8.
- [29] L.-G. Hwa, J.-G. Shiau, et S.-P. Szu, "Polarized Raman scattering in lanthanum gallogermanate glasses", *Journal of Non-Crystalline Solids*, vol. 249, n° 1, p. 55-61, juill. 1999, doi: 10.1016/S0022-3093(99)00300-2.
- [30] L.-G. Hwa, Y.-R. Chang, et S.-P. Szu, "Optical and physical properties of lanthanum gallogermanate glasses", *Journal of Non-Crystalline Solids*, vol. 231, n° 3, p. 222-226, août 1998, doi: 10.1016/S0022-3093(98)00455-4.
- [31] Hwa, L.G., Chao, W.C. & Szu, S.P. "Temperature dependence of elastic moduli of lanthanum gallogermanate glasses", *Journal of Materials Science* **37**, 3423–3427 (2002). <https://doi.org/10.1023/A:1016550720293>
- [32] Hwa, LG., Lay, HY. & Szu, SP. "Elastic properties of lanthanum gallogermanate glasses", *Journal of Materials Science* **34**, 5999–6002 (1999). <https://doi.org/10.1023/A:1004736913276>
- [33] J. M. Jewell, P. L. Higby, et I. D. Aggarwal, "Properties of BaO-R₂O₃- Ga₂O₃-GeO₂ (R = Y, Al, La, and Gd) Glasses", *J American Ceramic Society*, vol. 77, n° 3, p. 697-700, mars 1994, doi: 10.1111/j.1151-2916.1994.tb05351.x.
- [34] L. G. Hwa, Y. R. Chang, et W. C. Chao, "Infrared spectra of lanthanum gallogermanate glasses", *Materials Chemistry and Physics*, vol. 85, n° 1, p. 158-162, mai 2004, doi: 10.1016/j.matchemphys.2003.12.021.
- [35] Luo, Y.-R. (2007). "Comprehensive Handbook of Chemical Bond Energies" (1st ed.), CRC Press. <https://doi.org/10.1201/9781420007282>
- [36] T. Skopak *et al.*, "Structure and Properties of Gallium-Rich Sodium Germano-Gallate Glasses", *The Journal of Physical Chemistry C*, vol. 123, n° 2, p. 1370-1378, janv. 2019, doi: 10.1021/acs.jpcc.8b08632.

- [37] G. S. Henderson, L. G. Soltay, et H. M. Wang, "Q speciation in alkali germanate glasses", *Journal of Non-Crystalline Solids*, vol. 356, n° 44-49, p. 2480-2485, oct. 2010, doi: 10.1016/j.jnoncrysol.2010.03.023.
- [38] D. M. McKeown et C. I. Merzbacher, "Raman spectroscopic studies of BaO-Ga₂O₃-GeO₂ glasses", *Journal of Non-Crystalline Solids*, vol. 183, n° 1-2, p. 61-72, avr. 1995, doi: 10.1016/0022-3093(94)00648-2.
- [39] E. I. Kamitsos, Y. D. Yiannopoulos, M. A. Karakassides, G. D. Chryssikos, et H. Jain, "Raman and Infrared Structural Investigation of xRb₂O·(1 - x)GeO₂ Glasses", *J. Phys. Chem.*, vol. 100, n° 28, p. 11755-11765, janv. 1996, doi: 10.1021/jp960434+.
- [40] K. Yoshimoto, A. Masuno, M. Ueda, H. Inoue, H. Yamamoto, et T. Kawashima, "Low phonon energies and wideband optical windows of La₂O₃-Ga₂O₃ glasses prepared using an aerodynamic levitation technique", *Scientific Reports*, vol. 7, n° 1, déc. 2017, doi: 10.1038/srep45600.
- [41] K. Yoshimoto *et al.*, "Principal Vibration Modes of the La₂O₃-Ga₂O₃ Binary Glass Originated from Diverse Coordination Environments of Oxygen Atoms", *J. Phys. Chem. B*, vol. 124, n° 24, p. 5056-5066, juin 2020, doi: 10.1021/acs.jpcc.0c02147.
- [42] J. Hanuza et M. Andruszkiewicz, "Phonon properties and normal coordinate analysis of gallium-oxygen core in BaLaGa₃O₇ crystal", *Spectrochimica Acta Part A: Molecular and Biomolecular Spectroscopy*, vol. 51, n° 5, p. 869-881, mai 1995, doi: 10.1016/0584-8539(94)01235-9.